Modelling of Turbulent Premixed Stratified Combustion with Multiple Mapping Conditioning Mixing Model

C. Straub[1]*, A. Kronenburg[1], O.T. Stein[1], G. Kuenne[2], K. Vogiatzaki[3]

[1] Institut für Technische Verbrennung, Universität Stuttgart, Herdweg 51, 70174 Stuttgart, Germany
[2] Institute of Energy and Power Plant Technology, TU Darmstadt, Jovanka-Bontschits-Strasse 2, 64287 Darmstadt, Germany
[3] School of Computing, Engineering and Mathematics, University of Brighton, Lewes road, Brighton BN2 4GJ, UK

Abstract

A hybrid Euler/Lagrange approach is used to model stratified lean premixed combustion in a turbulent flow. Large eddy simulations (LES) are coupled with an artificially thickened flame (ATF) approach for the computation of the reaction progress variable. This approach is combined with a sparse Lagrangian particle method for the modelling of the inner flame structure. A multiple mapping conditioning (MMC) mixing model is applied to prevent direct mixing across the flame front. Predicted flame structures are compared with measurements of a stratified premixed laboratory flame yielding good agreement and demonstrating the model's capability to predict relatively thin flames and to approximate a flamelet-like inner flame structure.

Introduction

Lean premixed combustion is one of the most favourable combustion modes for applications of engineering interest due to its low propensity to soot and its potentially very low NO_x emissions. Despite the apparent advantages, lean premixed combustion is not always easy to realize due to inherent combustion instabilities and the necessity to increase the fuel concentration locally. In order to gain comprehensive information on the physics numerical models and experiments play an important role. The Darmstadt Turbulent Stratified Flame (TSF) series [1] provides physical insights for model development and serves as benchmark for code and model validation. One rather popular choice for the modelling of sub-grid turbulence-chemistry interactions is the flamelet model. Kuenne et al. [2] investigated premixed combustion by applying the artificially thickened flame (ATF) model coupled with the flamelet generated manifold (FGM) approach. Any flamelet model, including ATF-FGM, does not allow for any departures from the flamelet structure. The widening of the flame by the ATF model is rather artificial and a model extension that is expected to approximate the instantaneous, local flame structure for all premixed flame regimes is desired. Cleary and Klimenko [3] introduced generalized MMC as a particle mixing model for filtered density function (FDF) methods that were coupled with LES and applied to non-premixed turbulent flames. Sundaram et al. [4] investigated premixed combustion with probability density function (PDF) particle simulations using a multiple mapping conditioning (MMC) mixing model with 10000 particles for a 2-D problem. One of the inherent problems of a particle based method is mixing across the flame front which is unphysical and leads to an inaccurate prediction of the turbulent flame speed. This can be prevented by conditioning the mixing process on a reference variable that characterizes the relative position of the particle with respect to the flame. Here, we modify the approach followed by Sundaram et al. and use the LES filtered reaction progress variable as a reference scalar for conditioning. Effectively, we extend the ATF-FGM model by Kuenne et al. [2] by a sparse Lagrangian PDF method. The expression "sparse" states that fewer stochastic particles are used than there are computational cells. The model is referred to as "premixed MMC" in the remainder of the paper. The premixed MMC model is tested by comparison with a flame of the TSF series, namely TSF-A which features stratification but no shear. This specific flame has already served as a target flame for the validation of a variety of combustion models and a comparison can be found in [5].

Theory

The ATF-FGM model

In this work a large eddy simulation (LES) finite volume flow solver is applied to model turbulent stratified combustion. In addition to the governing equations for mass and momentum, the transport equations for $\widetilde{Y}_{CO_2}$ and the mixture fraction $\tilde{f}$ are solved, where $\tilde{\cdot}$ indicates Favre-filtering. Two-dimensional tabulated chemistry is used to model combustion by means of f and the CO_2 mass fraction as a progress variable. The table is generated by FGM [6]. With the choice of these two controlling variables stratification can be modelled. Our average LES grid resolution of $\Delta_x \approx 500\mu\mathrm{m} - 1\,\mathrm{mm}$ is too coarse to resolve the premixed flame front adequately and far smaller grid spacings would be needed. Therefore, the dynamic artificial thickening procedure is applied and coupled with the tabulated chemistry model [2]. The modified progress variable transport equation reads

*Corresponding author: carmen.straub@itv.uni-stuttgart.de

$$\frac{\partial \overline{\rho}\widetilde{Y}_{CO_2}}{\partial t} + \frac{\partial \overline{\rho}\widetilde{u}_i\widetilde{Y}_{CO_2}}{\partial x_i} = \frac{\partial}{\partial x_j}\left(\left[FE\overline{\rho}D_{CO_2} + (1-\Omega)\frac{\mu_t}{Sc_t}\right]\frac{\partial \widetilde{Y}_{CO_2}}{\partial x_j}\right) + \frac{E}{F}\dot{\omega}_{CO_2}, \tag{1}$$

where F is the thickening factor and E the efficiency function which accounts for unresolved flame wrinkling. The source term $\dot{\omega}_{CO_2}$ within the transport equation is given by the FGM table. The dynamic thickening approach [7] locates the flame via a flame sensor Ω which is defined as

$$\Omega = 16[\tilde{c}(1-\tilde{c})]^2 \quad \text{with} \quad \tilde{c} = \frac{\widetilde{Y}_{CO_2}}{Y^{\text{eq}}_{CO_2}}. \tag{2}$$

Here, $Y^{\text{eq}}_{CO_2}$ is the equilibrium value of $\widetilde{Y}_{CO_2}$ for a given mixture fraction. The thickening factor and the efficiency function act only within the preheat and reaction zones ($\Omega = 1$). Away from the flame ($\Omega = 0$) a turbulent viscosity approach is applied and $\Omega = 0$ leads to $F = 1$ since

$$F = 1 + (F_{\max} - 1)\Omega, \tag{3}$$

where $F_{\max}$ corresponds to the maximum thickening factor. It is given by

$$F_{\max} = \max\left(\frac{\sqrt[3]{\Delta_{x,1}\Delta_{x,2}\Delta_{x,3}}}{\Delta_{x,\max}}\right), \tag{4}$$

and represents a local (cell based) measure to ensure the desired resolution of the flame. The maximum grid size, $\Delta_{x,\max}$, is the maximum permissible grid size for a 1-D laminar flame simulation that ensures a deviation of the predicted laminar burning velocity from the accurate value by less than 10% [2]. The efficiency function required in Eq. (1) is computed via the model suggested by Charlette et al. [8] and a detailed derivation can be found therein. Similar to Eq. (1), the mixture fraction transport equation is modified and reads

$$\frac{\partial \overline{\rho}\tilde{f}}{\partial t} + \frac{\partial \overline{\rho}\widetilde{u}_i\tilde{f}}{\partial x_i} = \frac{\partial}{\partial x_j}\left(\left[FE\overline{\rho}D_{\tilde{f}} + (1-\Omega)\frac{\mu_t}{Sc_t}\right]\frac{\partial \tilde{f}}{\partial x_j}\right). \tag{5}$$

Lagrangian MMC model

The ATF-FGM model imposes a flamelet-like flame structure and we therefore extend the method by a FDF model to allow for deviations from this prescribed structure due to turbulence effects. In the context of LES an FDF approach describes the sub-filter probability density function of the fluctuating quantities. In this work its solution is obtained by a Lagrangian Monte Carlo formulation represented by a sparse particle distribution. The particles follow the LES velocity while molecular and turbulent diffusion are modelled by the particles' interactions. Here, the choice of the mixing model is important. Conventional FDF mixing models do not allow for flamelet-like solutions as particles can mix across the flame front. In this work the MMC mixing model is applied. The key feature of this model is the introduction of a reference variable which is used to condition the mixing of the particles and to enforce localness of the mixing particles in the reference space. Here, we extend the previous non-premixed MMC formulation by Cleary and Klimenko [3] to premixed conditions. Instead of using mixture fraction as a reference field, we use the thickened LES progress variable $\tilde{c}$. Mixing conditioned on this reference variable prevents particle pairs from mixing across the flame front. To enforce localness in reference space, the effective square distance between a particle pair (p and q) is introduced

$$\hat{d}^2_{p,q} = \sum_{i=1}^{3}\left(\sqrt{3}\frac{d^{p,q}_{x_i}}{r_m}\right) + \left(\frac{d^{p,q}_{\tilde{c}}}{c_m}\right), \tag{6}$$

and particle pairs are selected such that the average effective square distance is minimized. The distances between two particles p and q in physical and reference (here: progress variable) space are specified by $d^{p,q}_{x_i}$ and $d^{p,q}_{\tilde{c}}$, respectively. The characteristic mean mixing distance is r_m while c_m specifies the maximum mean distance of the particles in reference space. Both represent global model input parameters. Adapting again the non-premixed approach [3] r_m can be calculated from c_m as

$$r_m = C'\left(\frac{d\tilde{c}}{dn}\frac{\Delta_L^3}{\Delta_E^{2-D_f}}\frac{1}{c_m}\right)^{1/D_f}, \tag{7}$$

where $C' = 0.5$ is a model constant and $\frac{d\tilde{c}}{dn}$ is the maximum flame normal gradient of the thickened progress variable. Δ_L represents the (average) particle distance, Δ_E is the LES filter width and the fractal dimension is given by $D_f = 2.36$. Once the particle pairs are chosen they are mixed by the modified Curl's mixing model where two particles are mixed towards their common mean. The mixing time scale is modelled following [3]

$$\tau_L = C_L^{-1}C_E\frac{\beta d^2_{\tilde{c}}}{\widetilde{N}_{\tilde{c}}}, \tag{8}$$

where $C_L = 2.0$ and $\beta = 3$ are standard model constants. For premixed combustion we set $C_E = 1.0$. The scalar dissipation rate $\widetilde{N}_c$ is modelled by adapting the model by Dunstan et al. [9],

$$\widetilde{N}_c = \widetilde{D}_{\tilde{c}}F\nabla\tilde{c}\cdot F\nabla\tilde{c} + [1-\exp(-\theta_5\Delta/\delta_{th})] \times [\overbrace{2K_c(s_L/\delta_{th})}^{\text{dilatation}} + \overbrace{(C_3 - \tau C_4 Da_\Delta)\times(2u'_\Delta/3\Delta)}^{\text{strain rate}}] \overbrace{\tilde{c}(1-\tilde{c})/\beta_c}^{\text{reaction/molecular diss.}}, \tag{9}$$

where the model parameters are given as

$$\theta_5 = 0.75;\ K_c = 0.79\tau;\ \tau = (T_{ad} - T_u)/T_u; \tag{10}$$

$$C_3 = 1.5\sqrt{Ka_\Delta}/(1+\sqrt{Ka_\Delta}); \tag{11}$$

$$C_4 = 1.1/(1+Ka_\Delta)^{0.4} \text{ and } \beta_c = 2.4, \tag{12}$$

with $Ka_\Delta = (u'_\Delta/s_L)^{3/2}(\Delta/\delta_{th})^{-1/2}$ being the local Karlovitz number. In Eq. (9) the original expression [9] is modified by multiplying the progress variable gradients by the thickening factor F to approximate the correct values for the unthickened flame.

Note that in this work the thickened progress variable of the ATF-FGM approach, the LES velocity field and turbulent diffusivity are inputs for the sparse particle MMC method. Two-way coupling is not implemented in these first computations of MMC-LES for premixed flames, and the evolution of the LES fields is therefore not affected by the particles.

Case Setup

Flame Configuration

The setup of the TSF series consists of three staged concentric tubes placed in coflowing air. The flame is stabilized by the central pilot. The fuel is methane and different equivalence ratios within the tubes result in stratification. In this work the configuration TSF-A with stratification and no shear is investigated. The key geometrical data and operating conditions of the TSF-A are summarized in Table 1. The chosen operating conditions place the flame in the thin-reaction-zone regime which makes it an appropriate application for the suggested MMC model.

Table 1: Operating conditions of the reacting TSF-A.

Configuration	Pilot	Ring 1	Ring 2	Coflow
$r\,[\mathrm{mm}]$	7.4	18.5	30	300
$\phi\,[-]$	0.9	0.9	0.6	0.0
$U_{\mathrm{bulk}}\,[\mathrm{m/s}]$	10.0	10.0	10.0	0.1

Numerical Setup

The LES equations are solved in a Cartesian coordinate system using an OpenFOAM solver called mmcFoam [10] which is extended to account for the thickened flame model coupled with FGM tabulated chemistry. The computational domain extends $600\,\mathrm{mm}$ in radial direction. In axial direction the computational domain starts at $z = -20\,\mathrm{mm}$ and includes the pilot walls. The domain extends to $z = 296\,\mathrm{mm}$ in the axial direction. The radial and the axial directions of the domain are resolved by 67 and 192 cells, respectively. The LES grid consists of approximately 0.7 million cells. This leads to a cell size of $\Delta_x \approx 1.2\,\mathrm{mm}$ in the flame front at $z = 75\,\mathrm{mm}$. The eddy viscosity approach proposed by Smagorinsky [11] is used to model sub-grid viscosity. In order to describe realistic inflow boundary conditions, independent pipe flow simulations were conducted inside the two rings and specified at the rings' inlets. Artificial turbulence was generated by the approach described in [12] and assigned to the pilot stream. Approximately $300,000$ particles cover the computational domain which is about one stochastic particle for two LES cells. The number of stochastic MMC particles is controlled via an auxiliary mesh which is much coarser than the LES mesh. Every stochastic particle carries information on the composition scalar field and temperature. On the particles the reduced chemical mechanism DRM22 [13] with 24 species and 104 reactions is used. The key parameter of MMC, c_m, is chosen to equal $c_m = 0.03$ as for non-premixed flames. The corresponding r_m is computed according to Eq. (7). The transient behaviour is simulated with the ATF-FGM approach for approximately 23 flow through times based on the pilot bulk velocity. Then, the particles are initialized by the scalar fields from the final time step of the ATF-FGM solution and statistics are collected for further 2.5 flow through times. For one time step the computational cost for the particles is approximately 1.7 times the cost of the LES.

Results and Discussion

The performance of the ATF-FGM model as well as the premixed MMC model is investigated by comparison with measurements of TSF-A. Figure 1 displays mean axial velocity and root mean square (RMS) over the radial location at two different axial positions. The ATF-FGM

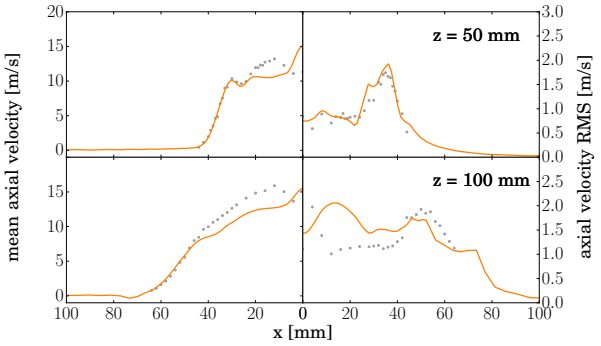

Figure 1: Radial profiles of mean axial velocity and RMS at different axial positions. Grey dots represent experimental data. Orange solid lines represent ATF-FGM solution.

results are represented by solid lines here and in the remainder of this work and compared to experimental data (symbols) [14, 1]. The predictions are generally in good agreement with the measurements. Except for the underprediction of the mean axial velocity at radial locations $r \in [10\,\mathrm{mm}, 30\,\mathrm{mm}]$ the results are comparable with the simulation data obtained in [5]. The results for mean radial velocity and RMS are of similar accuracy as the axial velocity, but not shown here due to space limitations.

Figure 2 displays mean temperature and RMS at four axial positions. During the computation the temperature on the LES grid is extracted from the FGM table and it is in good agreement with the experimental data. In [5] the influence of radiation was investigated. When radiation was neglected, the flame ignited further upstream which resulted in wider profiles of the mean temperature at upstream locations in comparison with the experimen-

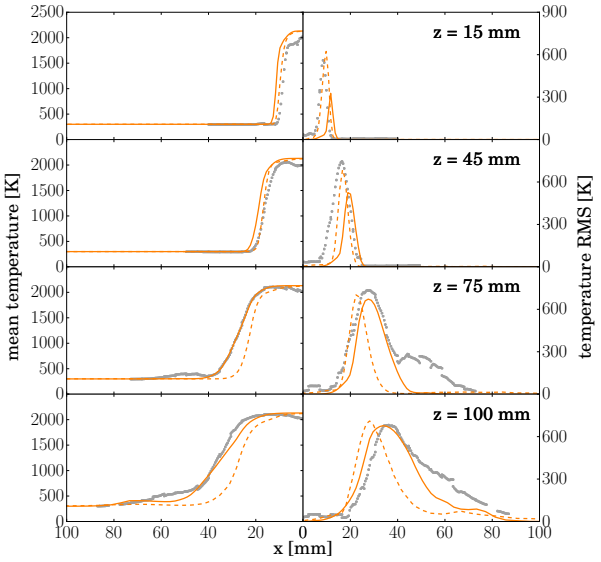

Figure 2: Radial profiles of mean temperature and RMS at different axial positions. Grey dots represent experimental data. Orange solid lines represent ATF-FGM solution. Orange dashed lines represent the Lagrangian solution.

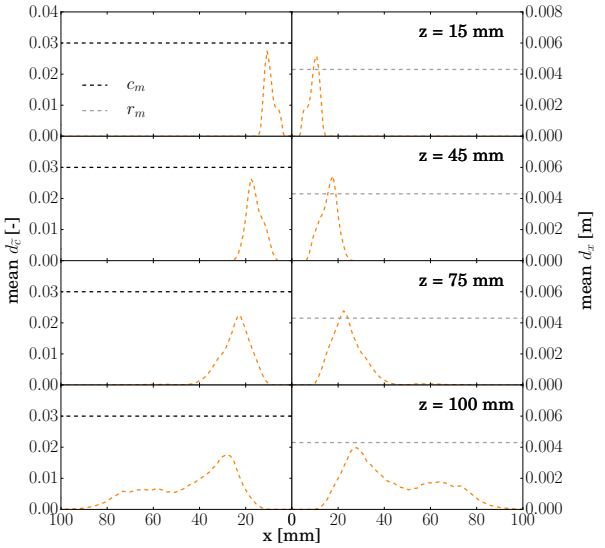

Figure 3: Radial profiles of mean $d_{\tilde{c}}$ and d_x at different axial positions. Additionally, the global parameters c_m and r_m are indicated by the dashed horizontal lines.

tal data. Here, the same observation for the ATF-FGM solution at $z = 15\,\mathrm{mm}$ and $z = 45\,\mathrm{mm}$ can likely be attributed to this effect too. The peak value of the ATF-FGM temperature RMS is underpredicted upstream but matches the experimental data fairly well when moving downstream. Underprediction of the temperature fluctuations is expected for the ATF-FGM model due to the artificial thickening of the flame which is supposed to be improved by the FDF solution. The Lagrangian solution is represented by dashed lines here and in the remainder of this work. The mean Lagrangian temperature in Fig. 2 approximately follows the mean Eulerian temperature. At $z = 15\,\mathrm{mm}$ and $z = 45\,\mathrm{mm}$ the flame position predicted by the particles is slightly shifted further inwards in comparison with the Eulerian solution. This effect is more pronounced at $z = 75\,\mathrm{mm}$ and $z = 100\,\mathrm{mm}$. The temperature RMS based on the particle quantities is increased in comparison with the Eulerian solution at the first axial locations and the level of the maximum fluctuation is close to the measured RMS. As the flame thickness on the particles is decreased, an increased temperature RMS is expected. At locations further downstream the maximum fluctuation is shifted inward due to the (mean) flame position on the particles. It should be noted that the increased LES temperature RMS at downstream locations and the increased temperature fluctuations from the particle quantities rather upstream can be fortuitous which needs further model investigation.

Figure 3 shows the mean distance of mixing particles in reference space $d_{\tilde{c}}$ and the mean distance in physical space d_x over radial location at various axial positions. These profiles illustrate where mixing takes place within the domain. The peaks of the mean mixing distance in reference space and in physical space align with the mean flame position, see Fig. 2. Consequently, the peaks get shifted outwards further downstream. At $z = 15\,\mathrm{mm}$ the maximum mean $d_{\tilde{c}}$ is of the order of the prescribed value of $c_m = 0.03$. The same holds for d_x. This demonstrates the correct implementation of the model. Further downstream, lower values of the maximum $d_{\tilde{c}}$ and d_x can be observed since the scalar gradient decreases. Moving towards the centerline both profiles tend to zero which is equivalent to no mixing. The same tendency is observed for larger radii (except at $z = 100\,\mathrm{mm}$). Due to the absence of mixing e.g. at $z = 15\,\mathrm{mm}$ and $r > 15\,\mathrm{mm}$ particles between ring 2 and the coflow are not mixed. This is an artefact of the current MMC implementation and indicates the need for an additional conditioning of the mixing process on equivalence ratio in these regions of the flame in order to account for stratification. At $z = 100\,\mathrm{mm}$ a second peak arises. This peak is attributed to initial transient effects which persist for a considerable time due to the very low coflow velocity of $U_{\mathrm{co}} = 0.1\,\mathrm{m/s}$. This peak is expected to vanish for longer sampling times.

In Fig. 4 the flame structure on the particles, as represented by temperature, is plotted versus the thickened progress variable. While the progress variable ranges from zero to one, the temperature change on the particles occurs over a more narrow range, i.e. the flame on the particles is significantly thinner in comparison to the LES solution and flamelet-like. The particle solution in Fig. 4 is shifted to the right and this becomes more pronounced at $z = 100\,\mathrm{mm}$. The mean location of the flame on the particles is not the same as the LES flame position, which is consistent with Fig. 2 where the Lagrangian solution diverges from the LES solution at $z = 100\,\mathrm{mm}$.

Figure 5 shows scatter data of OH mass fraction ver-

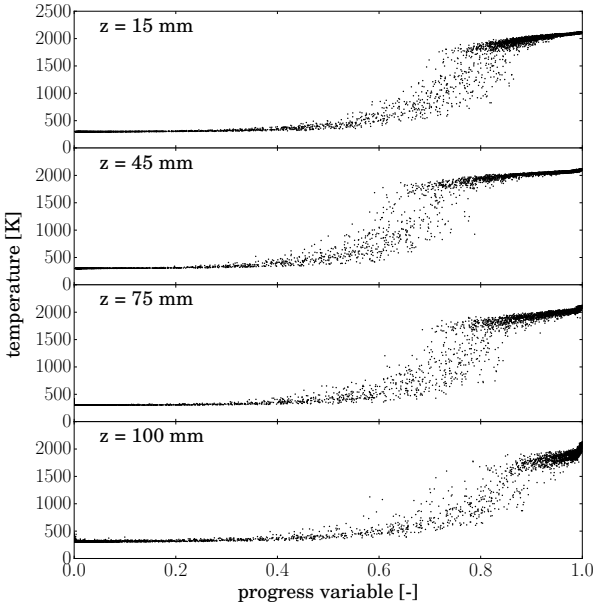

Figure 4: Scatterplot temperature T versus the thickened progress variable $\tilde{c}$ at different axial positions.

sus CO_2 mass fraction from the Lagrangian particles at different axial positions. The particles are coloured by

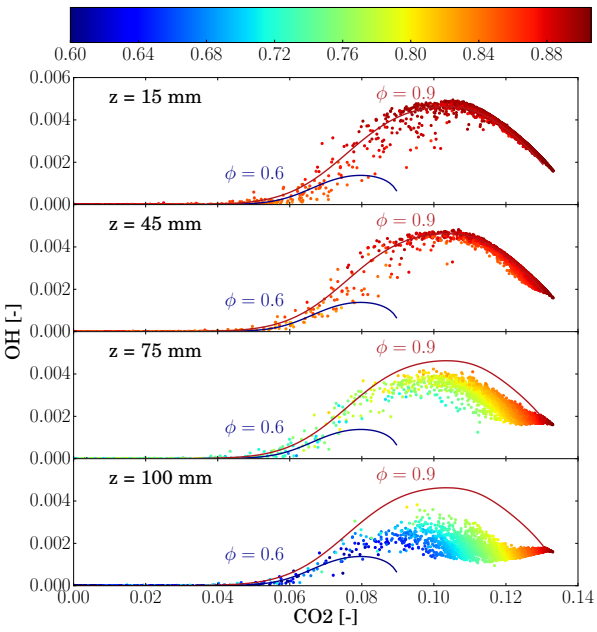

Figure 5: Scatterplot of mass fraction of OH versus mass fraction of CO_2 coloured by equivalence ratio ϕ at different axial positions. The solid lines are given by the FGM table for different equivalence ratios, namely $\phi = 0.6$ and $\phi = 0.9$.

equivalence ratio $\phi \in [0.6, 0.9]$, where the minimum and maximum values of this range are given by the equivalence ratios in the different rings. Additionally, the solid lines depict the flamelet solution of the FGM table for the two bounding equivalence ratios $\phi = 0.9$ and $\phi = 0.6$. Near the flame base, the particle solution seems to follow the flamelet solution quite closely indicating that MMC can preserve the flamelet structure. This is particularly true for high CO_2 values, i.e. in the reactive part of the premixed flame. Within the preheat zone, i.e. for smaller values of CO_2, the scatter increases indicating a deviation from the flamelet solution which can be expected for the thin flame regime. These observations may demonstrate that MMC is capable of predicting the different flame regimes, however, further parameter studies are needed to separate possible effects of (unphysical) mixing across the flame zone inherent in PDF methods from (accurate) predictions of flame broadening due to turbulence. Further downstream, fluctuations seem to abate, the particles' composition is close to their fully burned solution and the process is dominated by mixing of the hot products with the colder surroundings, i.e. the composition moves along the mixing line between a fully burnt state and air.

Conclusions

This work is a first application of sparse-Lagrangian MMC to premixed combustion. An LES solution for the turbulent stratified flame TSF-A is obtained by the ATF-FGM model. For modelling the inner flame structure, we use a sparse filtered density function model which is coupled to the ATF-FGM approach. The FDF approach applies the MMC mixing model to enforce localness in composition space. Model predictions are compared with experimental data. The ATF-FGM results of velocity and temperature compare well with measurements. The Lagrangian solution follows mostly the LES solution, but provides slightly more narrow profiles. Conditional plots of temperature versus filtered progress variable show a decreased flame thickness on the particles. The particle data illustrate a flamelet-like solution as a result of conditional mixing. Scatter data of the particles' OH versus CO_2 provide additional information on the flame structure. The flamelet-like character of the flame is corroborated in the reaction zone of the flame while some deviation from the flamelet solution can be observed in the preheat zone. Additional sensitivity studies are required to establish the nature of these deviations and the influence of the model parameters on flame structure.

Acknowledgements

The financial support by Deutsche Forschungsgemeinschaft (DFG) (grant numbers KR3684/7-1 and JA544/41-1) is acknowledged. The authors would like to thank A. Dreizler for providing the experimental data for the TSF series.

References

[1] F. Seffrin, F. Fuest, D. Geyer, A. Dreizler, Flow field studies of a new series of turbulent premixed stratified flames, Combustion and Flame 157 (2) (2010) 384–396.

[2] G. Kuenne, A. Ketelheun, J. Janicka, LES modeling of premixed combustion using a thickened flame approach coupled with FGM tabulated chemistry, Combustion and Flame 158 (9) (2011) 1750–1767.

[3] M. J. Cleary, A. Y. Klimenko, A detailed quantitative analysis of sparse-Lagrangian filtered density function simulations in constant and variable density reacting jet flows, Physics of Fluids 23 (11) (2011) 115102.

[4] B. Sundaram, A. Klimenko, A PDF approach to thin premixed flamelets using multiple mapping conditioning, Proceedings of the Combustion Institute.

[5] B. Fiorina, R. Mercier, G. Kuenne, A. Ketelheun, A. Avdić, J. Janicka, D. Geyer, A. Dreizler, E. Alenius, C. Duwig, P. Trisjono, K. Kleinheinz, S. Kang, H. Pitsch, F. Proch, F. Cavallo Marincola, A. Kempf, Challenging modeling strategies for LES of non-adiabatic turbulent stratified combustion, Combustion and Flame 162 (11) (2015) 4264–4282.

[6] J. Oijen, L. Goey, Modelling of premixed laminar flames using flamelet-generated manifolds, Combustion Science and Technology 161 (1) (2000) 113–137.

[7] L. Durand, W. Polifke, Implementation of the Thickened Flame Model for Large Eddy Simulation of Turbulent Premixed Combustion in a Commercial Solver, in: Volume 2: Turbo Expo 2007, ASME, 2007, pp. 869–878.

[8] F. Charlette, C. Meneveau, D. Veynante, A power-law flame wrinkling model for LES of premixed turbulent combustion Part I: non-dynamic formulation and initial tests, Combustion and Flame 131 (1-2) (2002) 159–180.

[9] T. D. Dunstan, Y. Minamoto, N. Chakraborty, N. Swaminathan, Scalar dissipation rate modelling for large eddy simulation of turbulent premixed flames, Proceedings of the Combustion Institute 34 (1) (2013) 1193–1201.

[10] B. Sundaram, A. Y. Klimenko, M. J. Cleary, Y. Ge, A direct approach to generalised multiple mapping conditioning for selected turbulent diffusion flame cases, Combustion Theory and Modelling 20 (4) (2016) 735–764.

[11] J. Smagorinsky, General circulation experiments with the primitive equations, Monthly Weather Review 91 (3) (1963) 99–164.

[12] A. Kempf, M. Klein, J. Janicka, Efficient Generation of Initial- and Inflow-Conditions for Transient Turbulent Flows in Arbitrary Geometries, Flow, Turbulence and Combustion 74 (1) (2005) 67–84.

[13] A. Kazakov, M. Frenklach, Reduced Reaction Sets based on GRI-mech1.2, available at http://combustion.berkeley.edu/drm/.

[14] G. Kuenne, F. Seffrin, F. Fuest, T. Stahler, A. Ketelheun, D. Geyer, J. Janicka, A. Dreizler, Experimental and numerical analysis of a lean premixed stratified burner using 1D Raman/Rayleigh scattering and large eddy simulation, Combustion and Flame 159 (8) (2012) 2669–2689.